Supporting Information

Mechanically robust all-solid-state supercapacitor based on highly conductive double-network hydrogel electrolyte and $Ti_3C_2T_x$ MXene electrode with anti-freezing property

Junbo Peng[a], Manhua Zhou[a], Yafei Gao[a], Jianfeng Wang[a], Yanxia Cao[a], Wanjie Wang[a,*], Decheng Wu[b,*] and Yanyu Yang[a,*]

[a] College of Materials Science and Engineering, Zhengzhou University, Zhengzhou, Henan 450001, China.

[b] Department of Biomedical Engineering, Southern University of Science and Technology, Shenzhen, Guangdong 518055, China.

* Corresponding authors.

E-mails: wwj@zzu.edu.cn; wudc@sustech.edu.cn; yyyang@zzu.edu.cn

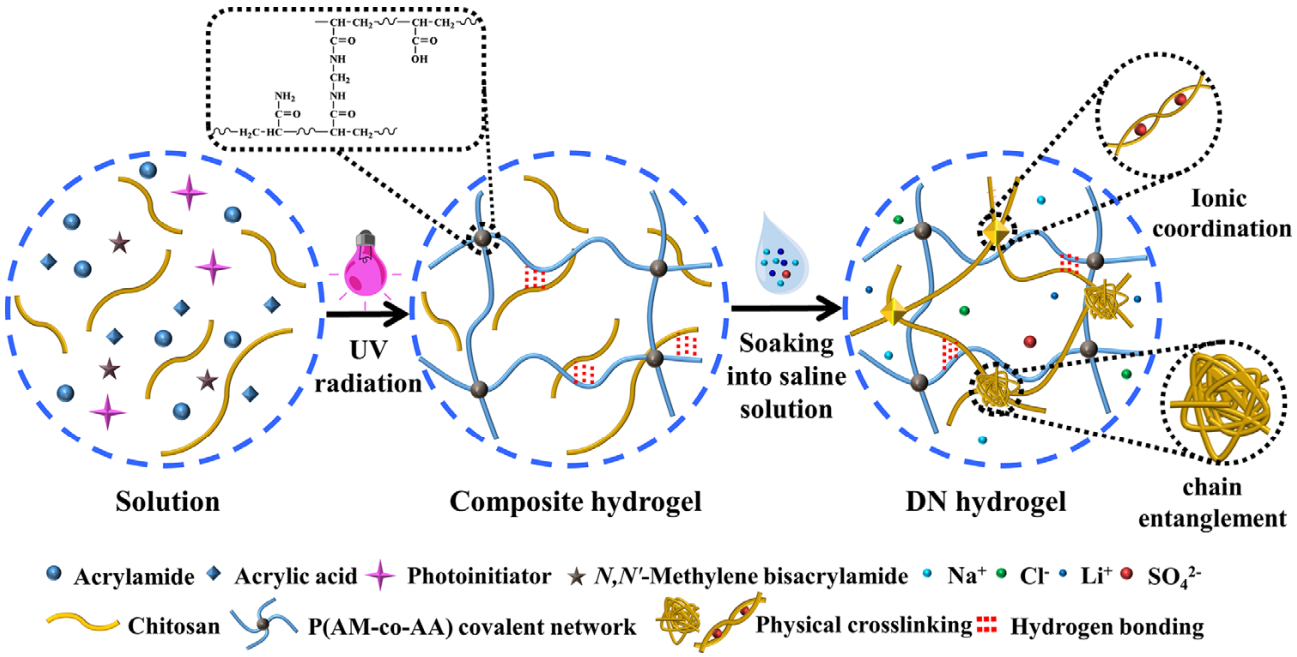

Fig. S1 Schematic illustration of preparation of the high-mechanical, ionic conductive and anti-freezing CS-P(AM-co-AA) DN hydrogel.

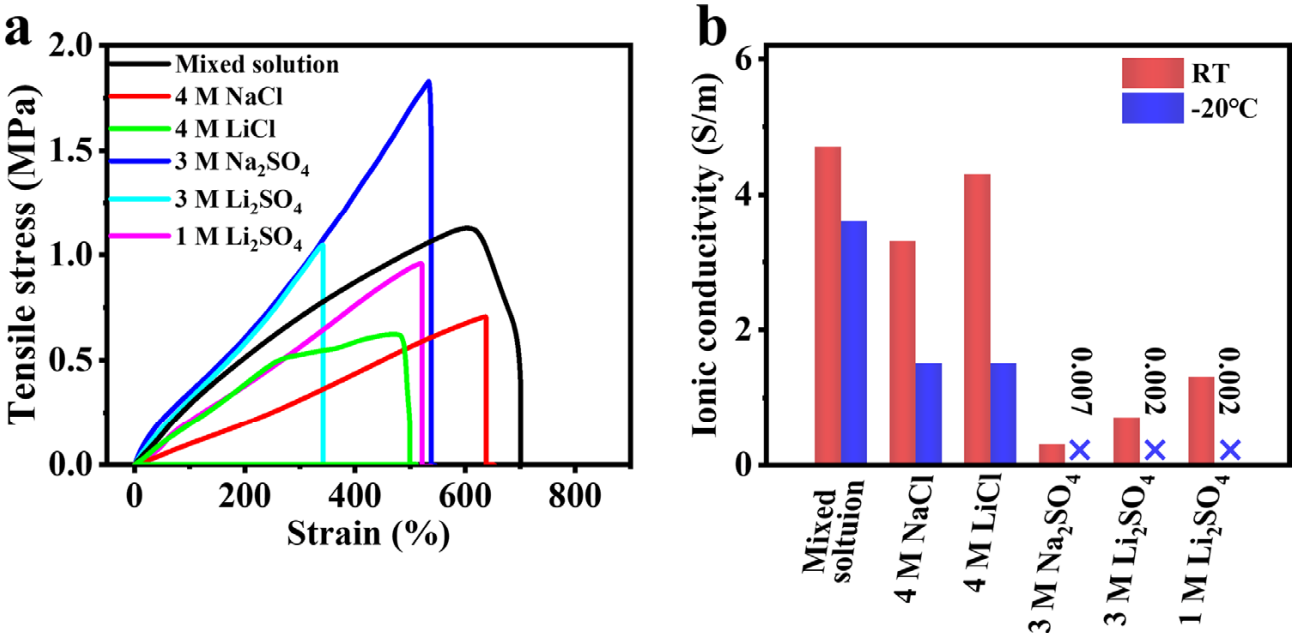

Fig. S2 Comparison of tensile curves and ionic conductivities of the CS-P(AM-co-AA) DN hydrogels prepared from mixed saline solution and control DN hydrogels prepared from single solution.

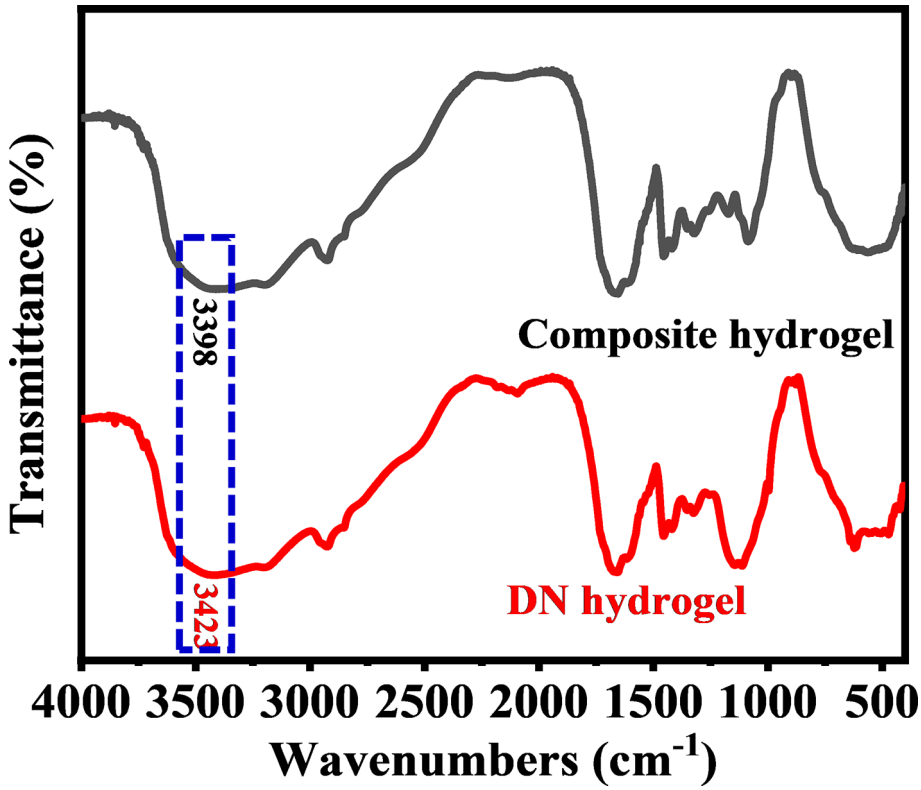

Fig. S3 FTIR spectra of CS-P(AM-co-AA) composite and DN hydrogels.

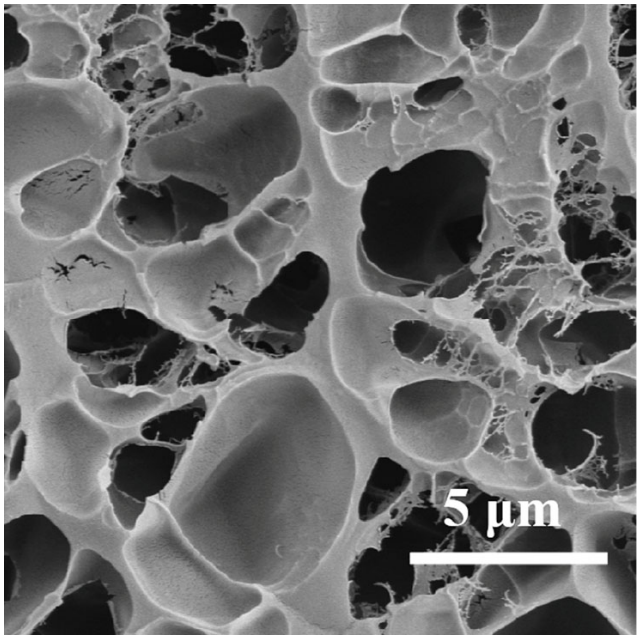

Fig. S4 SEM images of CS-P(AM-co-AA) composite hydrogel.

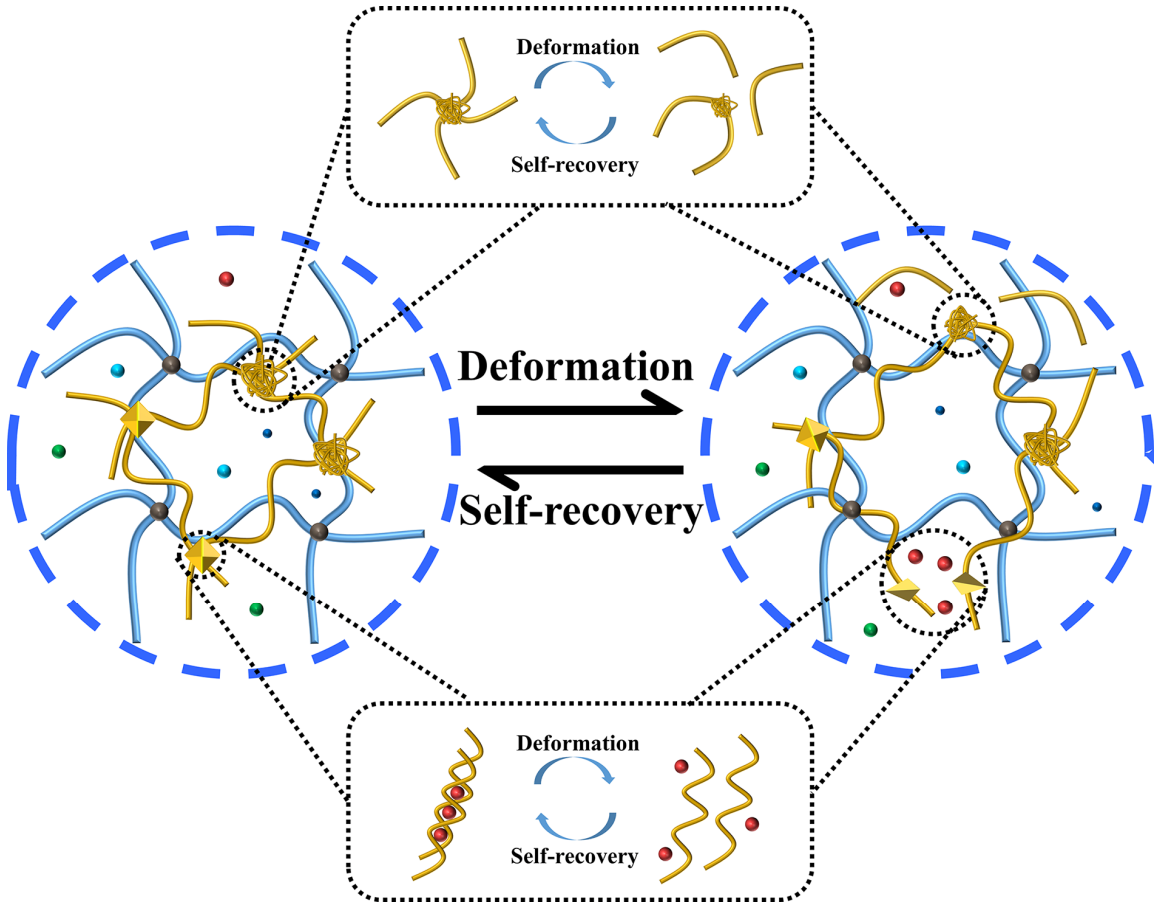

Fig. S5 Energy dissipation mechanism of the DN hydrogel.

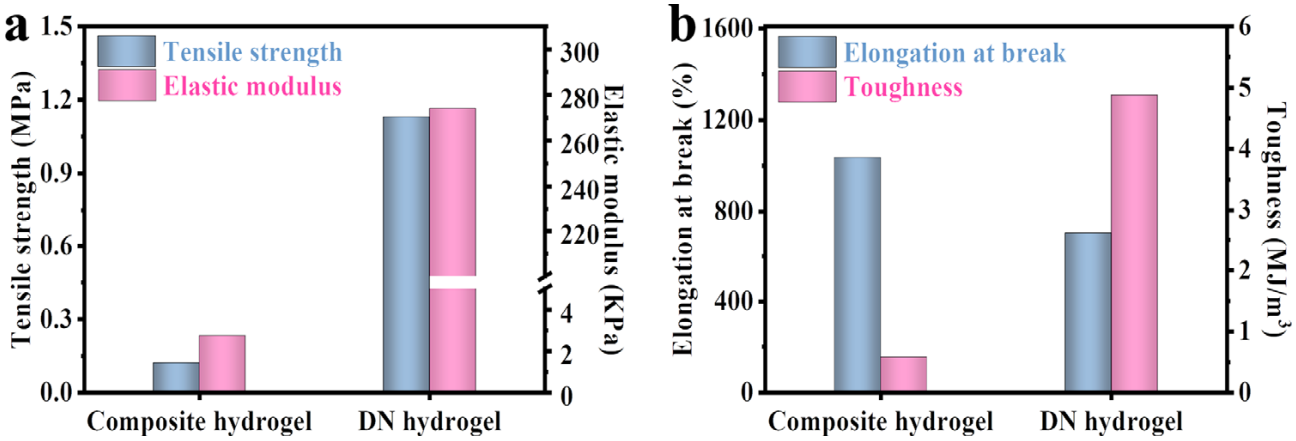

Fig. S6 (a) Elongation at break and tensile strength of the CS-P(AM-co-AA) composite and DN hydrogels. (b) Toughness and elastic modulus of the CS-P(AM-co-AA) composite and DN hydrogels.

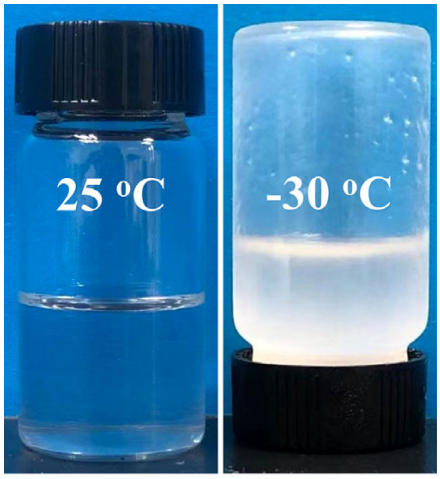

Fig. S7 Liquid state of the mixed saline solution (4 M NaCl and 1 M Li_2SO_4) at 25 and −30 ℃.

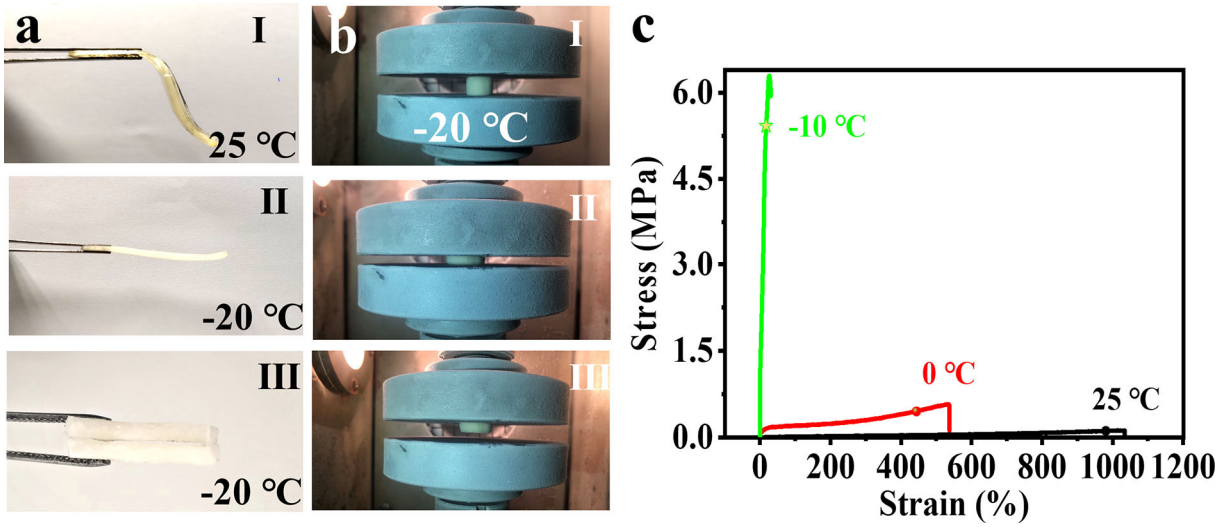

Fig. S8 (a) Optical images of the CS-P(AM-co-AA) composite hydrogel at (I) 25 and (II, III) −20 ℃. (b) compression-relaxation cycle at −20 ℃: (I) original state, (II) compressive state at strain of 50% and (III) restored-state after unloading. (c) Stress-strain curves of the CS-P(AM-co-AA) composite hydrogel at different temperatures.

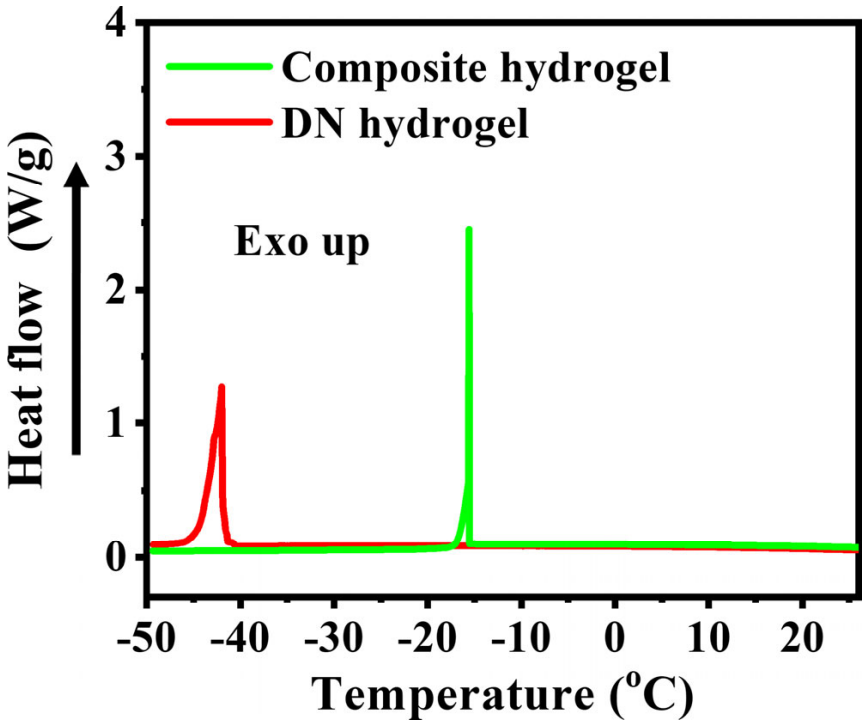

Fig. S9 DSC curve of the composite and DN hydrogels at the scan rate of 2 °C min^{-1}.

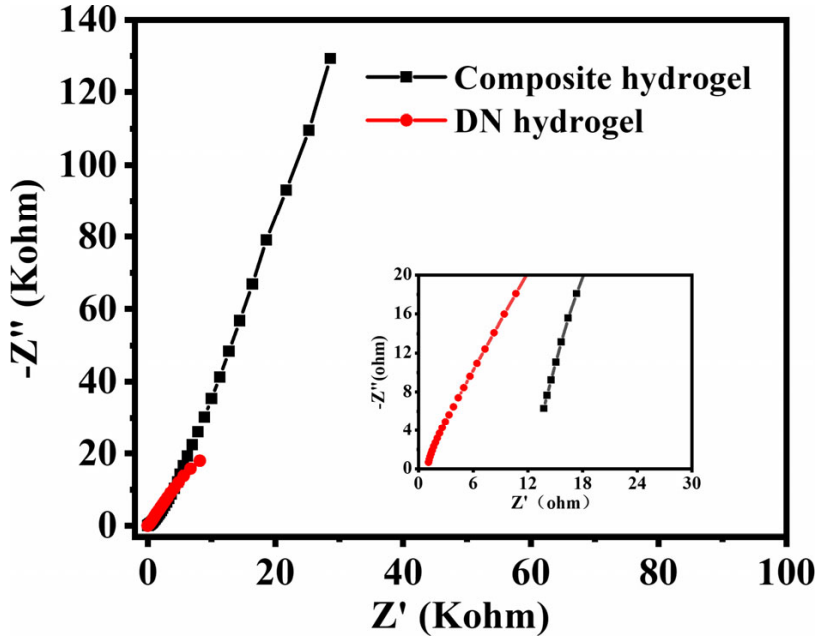

Fig. S10 Electrochemical impedance spectra of the CS-P(AM-co-AA) composite and DN hydrogels.

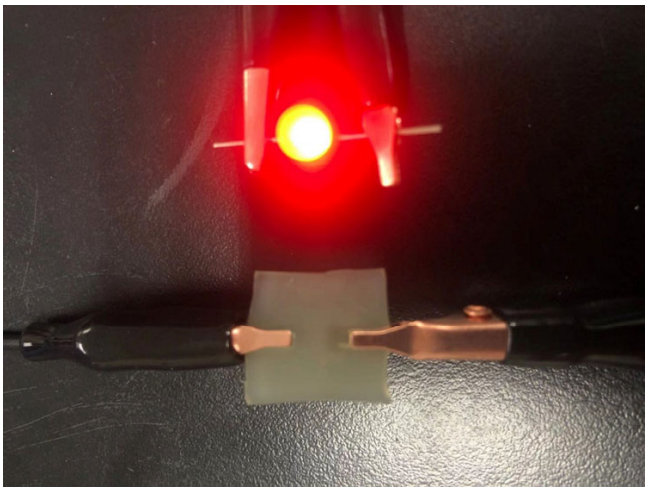

Fig. S11 CS-P(AM-co-AA) DN hydrogel serving as an ionic conductor in a closed circuit.

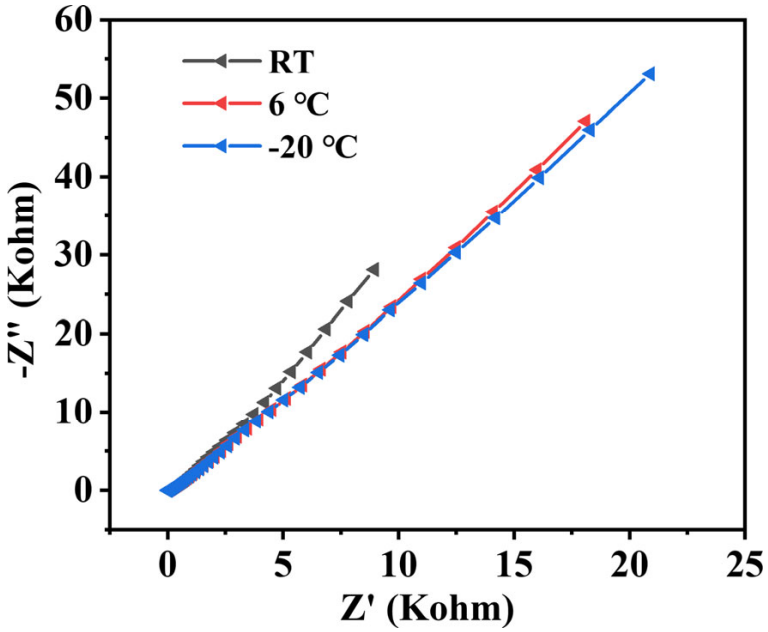

Fig. S12 Electrochemical impedance spectra of the CS-P(AM-co-AA) DN hydrogel at different temperatures.

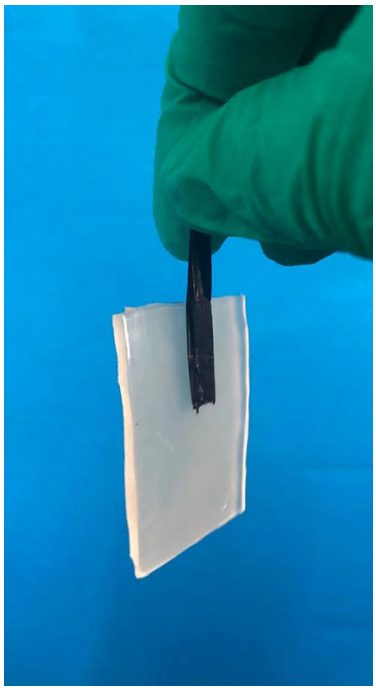

Fig. S13 Good adhesion between CNTs film current collector and hydrogel electrolyte due to hydrophilic interaction and hydrogen bonding.

Fig. S14 Thickness measurement of the MXene film.

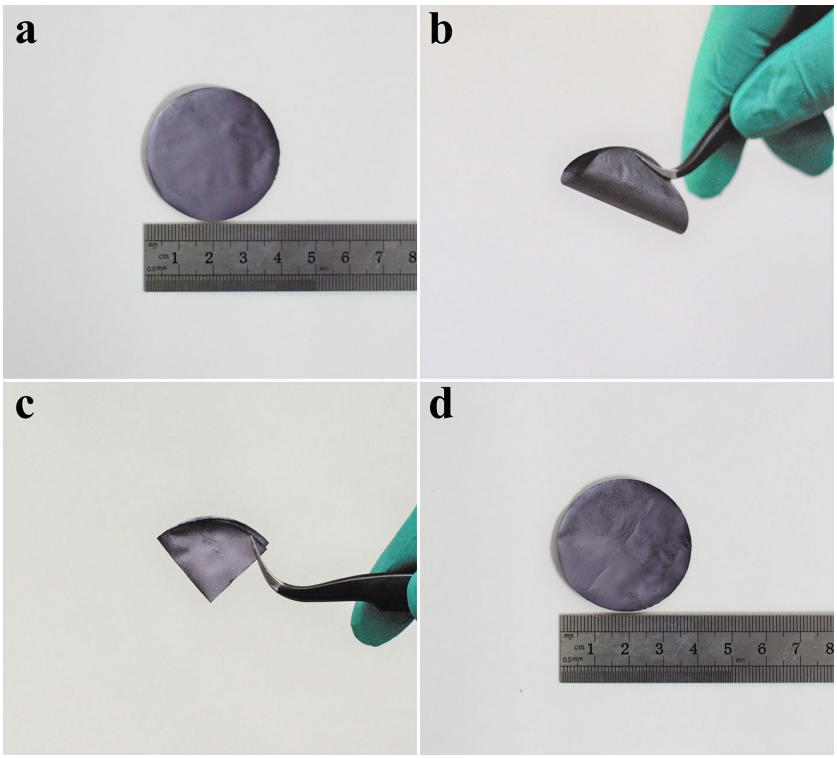

Fig. S15 Optical images of the MXene film upon various deformations. (a) Initial state, (b) bended state, (c) folded state and (d) recover state.

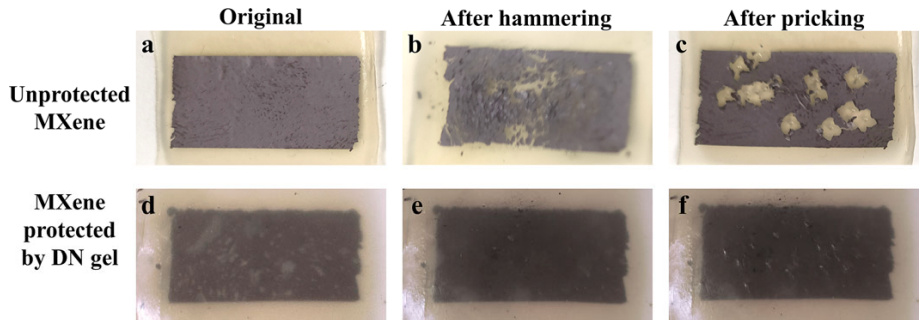

Fig. S16 (Top) Unprotected MXene and (bottle) protected MXene (a, d) before mechanical damage and after (b, e) hammering and (c, f) pricking.

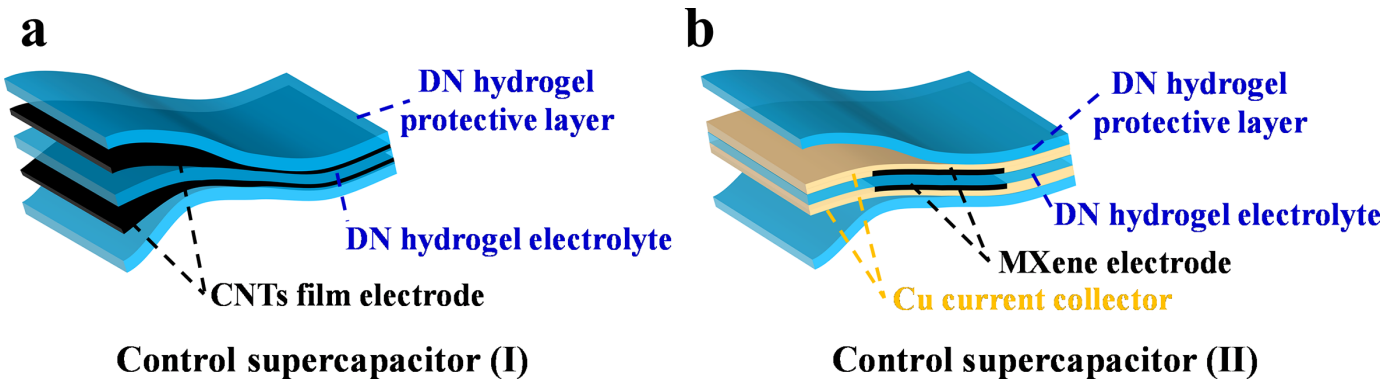

Fig. S17 Structural representation of two control supercapacitors.

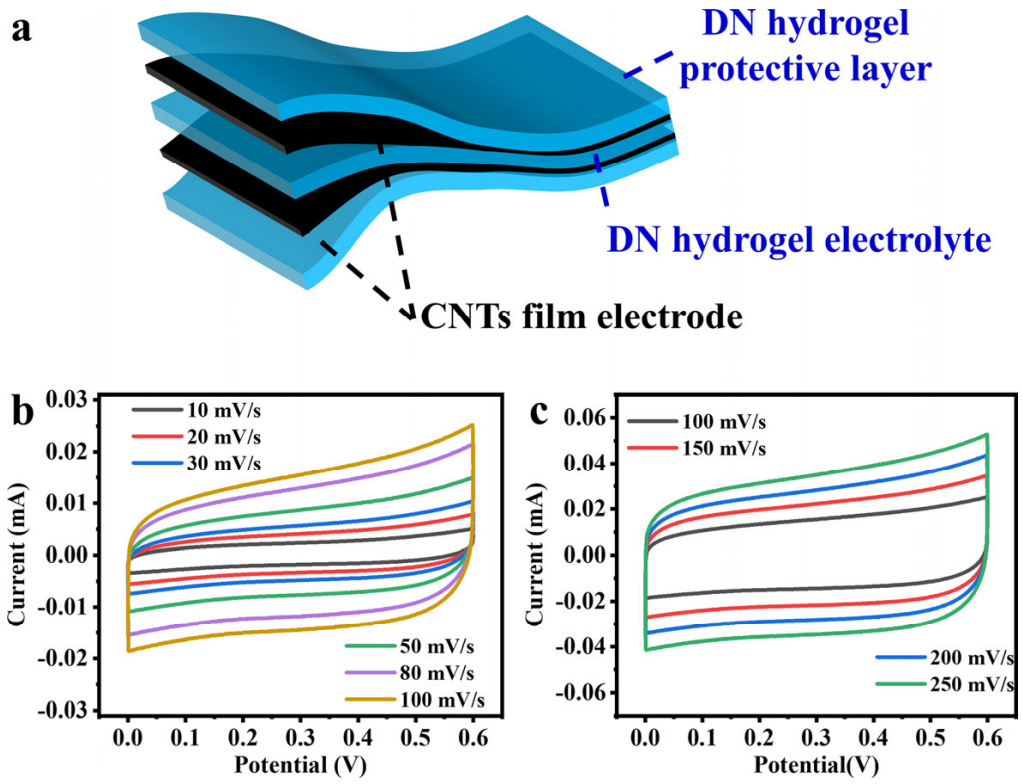

Fig. S18 (a) Structural representation of the control supercapacitor (I) and its CV curves at scan rate of (b) 10-100 and (c) 100-250 mV s^{-1}.

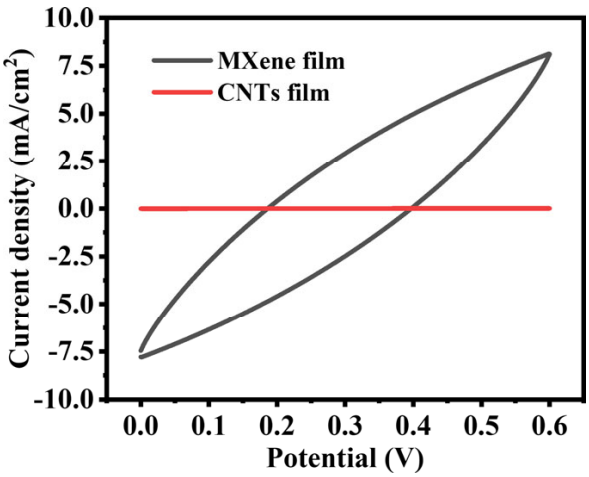

Fig. S19 Capacitive contrast of the supercapacitor with MXene film electrode and control supercapacitor (I) at scan rate of 100 mV s^{-1}.

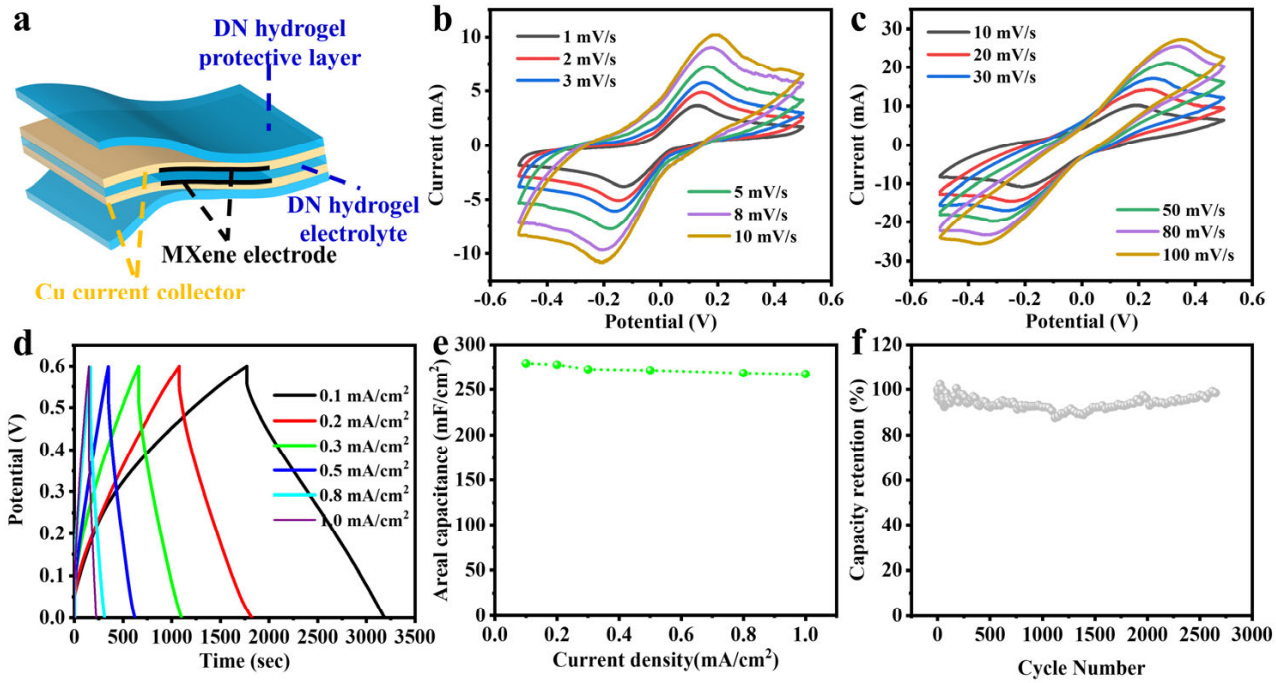

Fig. S20. Structural representation of the control supercapacitor (II) and electrochemical performance of the supercapacitor with Cu current collectors. (a) Structure of control supercapacitor. (II). CV curves at scan rate of (b) 1-10 and (c) 10-100 mV s^{-1}. (d) GCD curves at the current density of 0.1-1.0 mA cm^{-2}. (e) Areal capacitance at different current densities calculated from GCD curves. (f) Cyclic performance tested at the current density of 1 mA cm^{-2}.

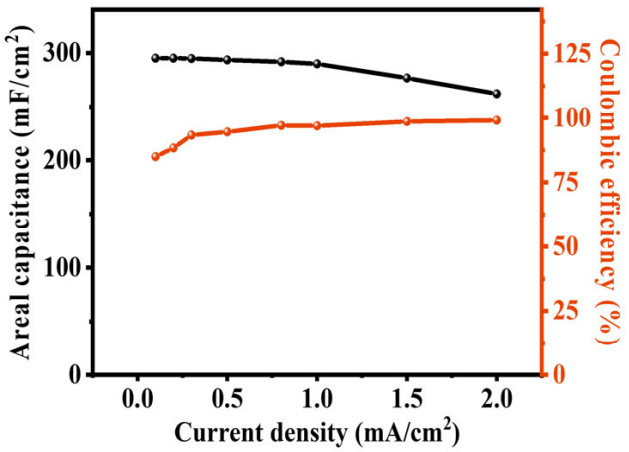

Fig. S21. Areal capacitance and coulombic efficiency of the assembled supercapacitor.

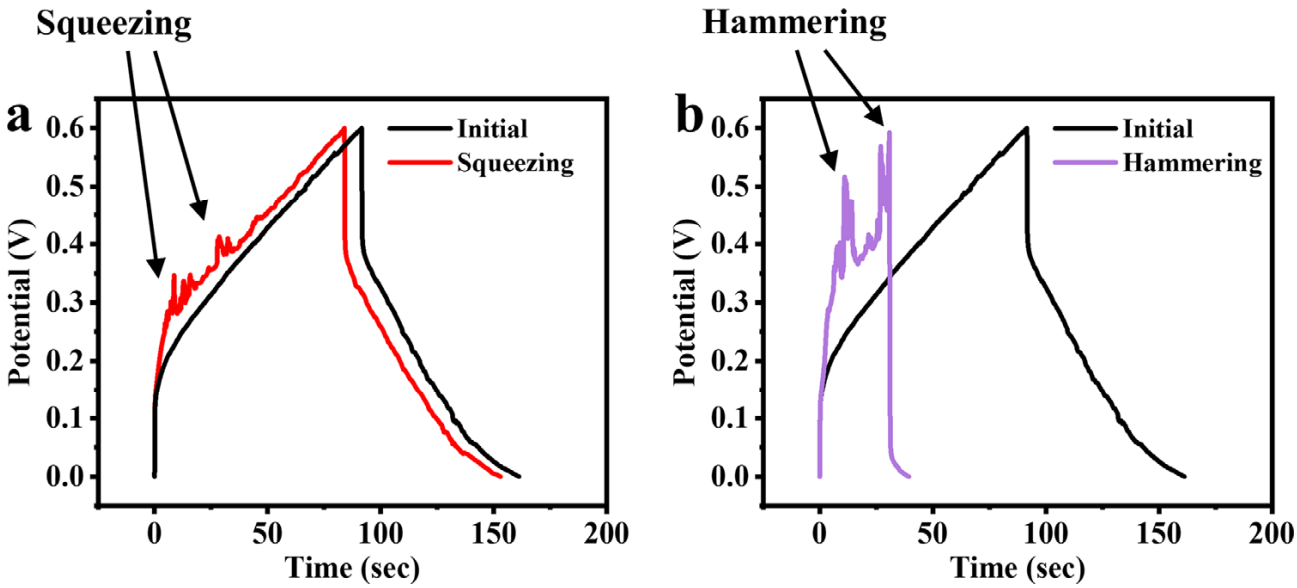

Fig. S22 (a) GCD curves of the control supercapacitor (II) before and during the dynamically squeezing process. (b) GCD curve of the control supercapacitor (II) before and during the dynamically hammering process.

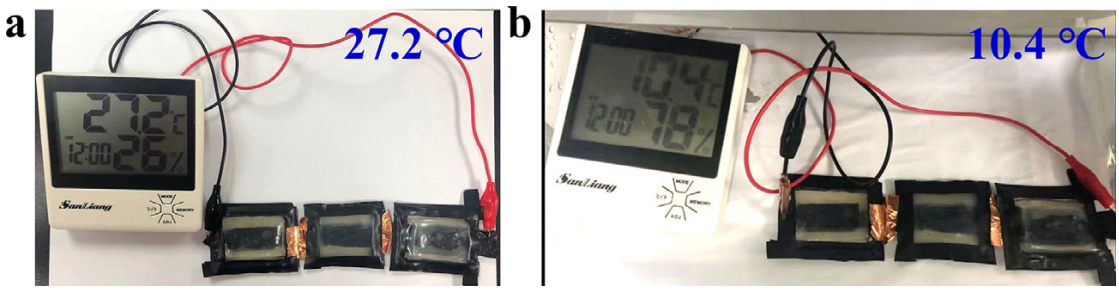

Fig. S23 Digital photos of a thermohygrometer activated by three supercapacitors connected in series at (a) 27.2 and (b) 10.4 ºC.

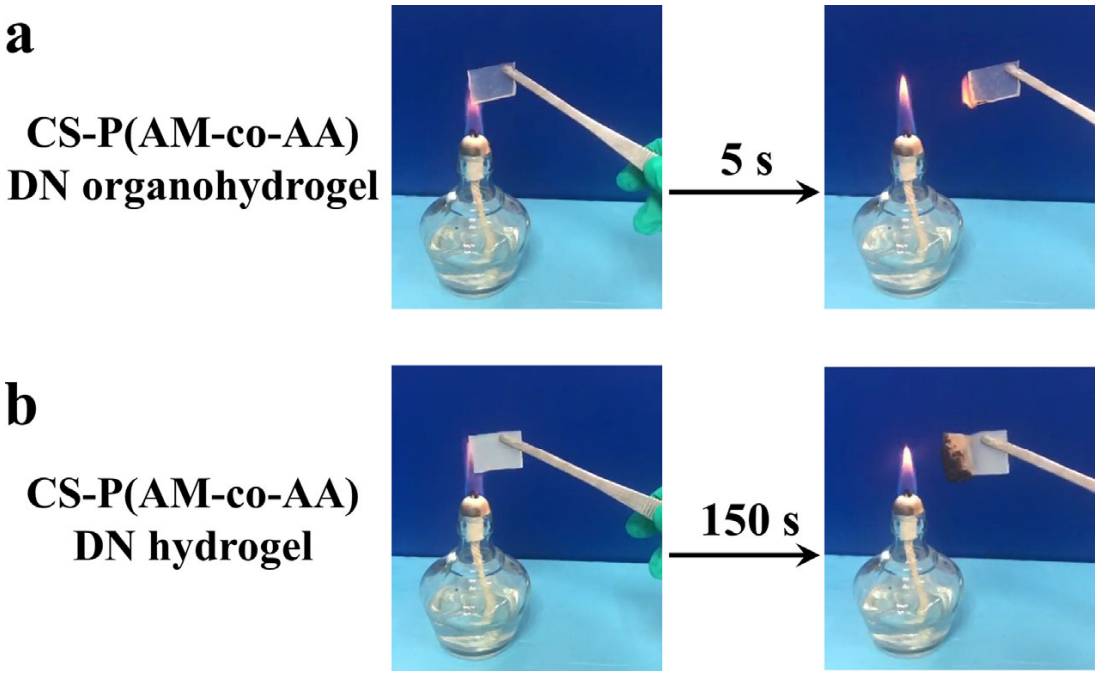

Fig. S24 Photographs of CS-P(AM-co-AA) DN (a) organohydrogel and (b) hydrogel combusted by flame.

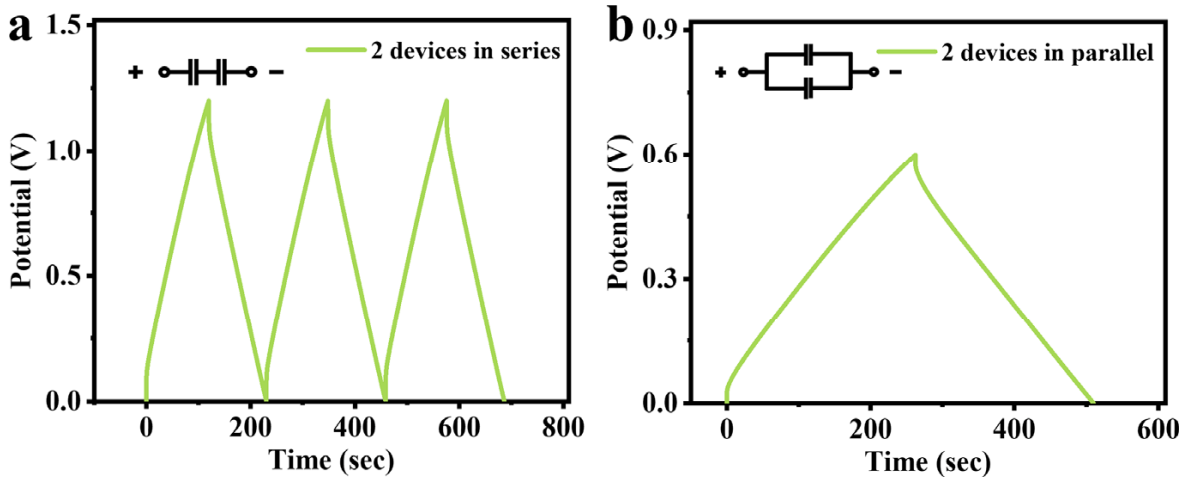

Fig. S25 GCD curves of two supercapacitors connected in (a) series and (b) parallel.

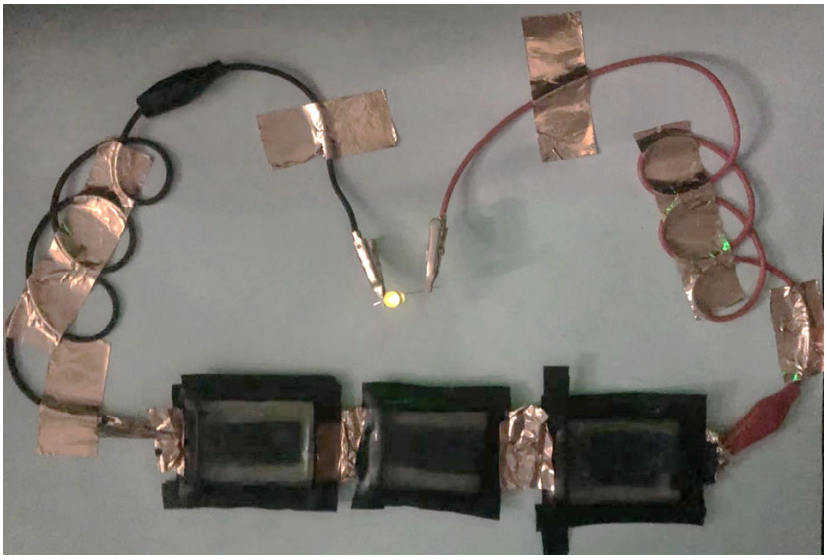

Fig. S26 Digital photo of a yellow LED light activated by three supercapacitors connected in series.

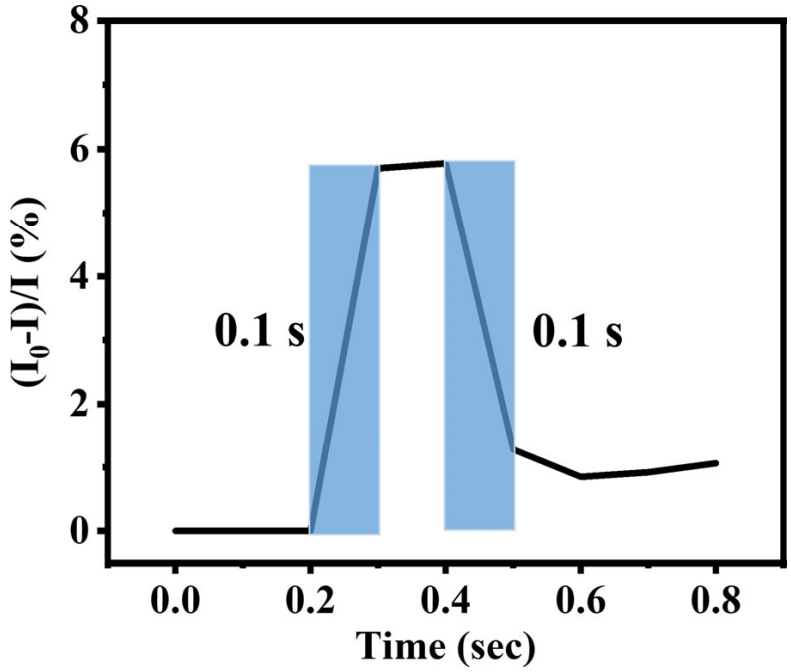

Fig. S27 Response time of DN hydrogel based strain sensor during loading and unloading process at tensile strain of 5%.